J|A|C|S
ARTICLES
Published on Web 12/21/2005

Host−Guest Complexes between an Aromatic Molecular Tweezer and Symmetric and Unsymmetric Dendrimers with a 4,4′-Bipyridinium Core

Vincenzo Balzani,*,† Heinz Bandmann,‡ Paola Ceroni,† Carlo Giansante,†
Uwe Hahn,§ Frank-Gerrit Klärner,*,‡ Ute Müller,§ Walter M. Müller,§
Carla Verhaelen,‡ Veronica Vicinelli,† and Fritz Vögtle*,§

Contribution from the Dipartimento di Chimica "G. Ciamician", Università di Bologna, Via Selmi 2, 40126 Bologna, Italy, Institut für Organische Chemie der Universität Duisburg-Essen, Campus Essen, Universitätsstrasse 5, 45117 Essen, Germany, and Kekulé-Institut für Organische Chemie und Biochemie der Universität Bonn, Gerhard-Domagk Strasse 1, 53121 Bonn, Germany

Received October 3, 2005; E-mail: vincenzo.balzani@unibo.it

Abstract: We have investigated the spectroscopic and electrochemical behavior of symmetric and unsymmetric first-, second-, and third-generation dendrimers comprising an electron-acceptor 4,4′-bipyridinium core (viologen type) and electron-donor 1,3-dimethyleneoxybenzene (Fréchet-type) dendrons. The quite strong fluorescence of the symmetrically and unsymmetrically disubstituted 1,3-dimethyleneoxybenzene units of the dendrons is completely quenched as a result of donor−acceptor interactions that are also evidenced by a low-energy tail in the absorption spectrum. In dichloromethane solution, the 4,4′-bipyridinium cores of the investigated dendrimers are hosted by a molecular tweezer comprising a naphthalene and four benzene components bridged by four methylene units. Host−guest formation causes the quenching of the tweezer fluorescence. The association constants, as measured from fluorescence and ^{1}H NMR titration plots, (i) are of the order of 10^4 M^{-1}, (ii) decrease on increasing dendrimer generation, and (iii) are slightly larger for the unsymmetric than for the symmetric dendrimer of the same generation. The analysis of the complexation-induced shifts of the temperature-dependent ^{1}H NMR signals of the host and guest protons confirms that the bipyridinium core is positioned inside the tweezer cavity and allows the conclusions that (i) shuttling of the tweezer from one to the other pyridinium ring is fast ($\Delta G^{\ddagger} < 10$ kcal/mol), (ii) in the case of the unsymmetric dendrimers, the less substituted pyridinium ring is preferentially complexed in apolar solvents, and (iii) complexation of the 4,4′-bipyridinium core proceeds by clipping for the symmetric dendrimers and by threading in the case of unsymmetric ones. Host−guest formation causes a displacement of the first reduction wave of the 4,4′-bipyridinium unit toward more negative potential values, whereas the second reduction wave is unaffected. These results show that the host−guest complexes between the tweezer and the dendrimers are stabilized by electron donor−acceptor interactions and can be reversibly assembled/disassembled by electrochemical stimulation.

Introduction

Dendrimers[1] are complex, yet well-defined, repetitively branched compounds with fractal structure reaching nanoscopic size. In some respects they resemble biocomponents like viruses, enzymes, and proteins.[2]

Because of their constitutional order, dendrimers can contain selected chemical units in predetermined sites of their structure (core, branches, periphery). Dendrimers containing photoactive[3] and redox-active[4] units are currently attracting much attention for a variety of applications which include light-harvesting antennae for artificial photosynthesis,[5] luminescent sensors with signal amplification,[6] light manipulation systems,[7] photocata-

† Università di Bologna.
‡ Universität Duisburg-Essen.
§ Universität Bonn.

(1) (a) Newkome, G. R.; Moorefield, C.; Vögtle, F. *Dendrimers and Dendrons: Concepts, Syntheses, Perspectives*; VCH: Weinheim, 2001. (b) Astruc, D. Special issue on Dendrimers and Nanoscience. *C. R. Chimie*, **2003**, *6* (8−10), 709.
(2) (a) Ottaviani, M. F.; Jockusch, S.; Turro, N. J.; Tomalia, D. A.; Barbon, A. *Langmuir* **2004**, *20*, 10238. (b) Liu, L.; Breslow, R. *J. Am. Chem. Soc.* **2003**, *125*, 12110.
(3) (a) Ceroni, P.; Bergamini, G.; Marchioni, F.; Balzani, V. *Prog. Polym. Sci.* **2005**, *30*, 453. (b) De Schryver, F. C.; Vosch, T.; Cotlet, M.; Van der Auweraer, M.; Muellen, K.; Hofkens, J. *Acc. Chem. Res.* **2005**, *38*, 514. (c) Balzani, V.; Ceroni, P.; Maestri, M.; Saudan, C.; Vicinelli, V. *Top. Curr. Chem.* **2003**, *228*, 159. (d) Nierengarten, J.-F.; Armaroli, N.; Accorsi, G.; Rio, Y.; Eckert, J. F. *Chem. Eur. J.* **2003**, *9*, 36.
(4) (a) Astruc, D.; Daniel, M.-C.; Ruiz, J. *Chem. Commun.* **2004**, 2637. (b) Astruc, D. *Pure Appl. Chem.* **2003**, *75*, 461. (c) Venturi, M.; Ceroni, P. *C. R. Chimie* **2003**, *6*, 935. (d) Cameron, C. S.; Gorman, C. B. *Adv. Funct. Mater.* **2002**, *12*, 17. (e) Campagna, S.; Di Pietro, C.; Loiseau, F.; Maubert, B.; McClenaghan, N. D.; Passalacqua, R.; Puntoriero, F.; Ricevuto, V.; Serroni, S. *Coord. Chem. Rev.* **2002**, *229*, 67.
(5) (a) Puntoriero, F.; Serroni, S.; Galletta, M.; Juris, A.; Licciardello, A.; Chiorboli, C.; Campagna, S.; Scandola, F. *ChemPhysChem* **2005**, *6*, 129. (b) Choi, M.-S.; Aida, T.; Luo, H.; Araki, Y.; Ito, O. *Angew. Chem., Int. Ed.* **2003**, *42*, 4060. (c) Jordens, S.; De Belder, G.; Lor, M.; Schweitzer, G.; Van der Auweraer, M.; Weil, T.; Reuther, E.; Müllen, K.; De Schryver, F. C. *Photochem. Photobiol. Sci.* **2003**, *2*, 177. (d) Hahn, U.; Gorka, M.; Vögtle, F.; Vicinelli, V.; Ceroni, P.; Maestri, M.; Balzani, V. *Angew. Chem., Int. Ed.* **2002**, *41*, 3595. (e) Serin, J. M.; Broumische, D. W.; Fréchet, J. M. J. *Chem. Commun.* **2002**, 2605.

lysts,[8] electrochemical sensors,[9] redox catalysts,[10] and molecular batteries.[11] Dendrimers with a single redox site as a core are the simplest examples of systems with an encapsulated redox center,[12] and their redox properties are usually modulated by the size and nature of the dendritic branches.[13]

Because of their large structures, dendrimers are extensively used as *host* molecules for a variety of metal ions[14] or molecules.[15] This concept has been further elaborated by incorporating single specific binding sites within the dendrimer, e.g. a cyclophane[16] or a cyclam[17] unit as a core. Dendrimers that can host metal ions or small molecules mimic in some way the behavior of proteins.

Despite their large structures, dendrimers can also be involved as *guests* in molecular recognition phenomena.[18] In such cases, the host species does not interact with the whole dendritic structure, but only with specific component units. Usually, the dendrimer-guest behavior is connected with the threading of dendritic branches by ring-shaped molecules.[19−21] Particularly active in this field is the group of Kaifer and co-workers,[18,22] who have prepared several dendrimers containing a single site as a potential guest unit and have investigated their adducts with β-cyclodextrin, cucurbituril, and bis-*para*-phenylene-34-crown-10.

When the potential guest unit constitutes the core of a symmetric dendrimer, host−guest formation requiring threading of ring-shaped hosts cannot take place. We have recently shown[23] that, in such a case, suitable tweezer-shaped molecules can be used to clip the dendritic core in dichloromethane solution.[24]

In this paper we extend our investigations to the host−guest systems obtained upon complexation of a molecular tweezer with two families of dendrimers. The tweezer used (**T** in Figure 1) comprises a naphthalene and four benzene components bridged by four methylene units and exhibits electron-donating properties.[25] The investigated dendrimers (Figure 1) consist of an electron-acceptor 4,4′-bipyridinium core with one (unsymmetric dendrimers, $\mathbf{D}n\mathbf{B}^{2+}$) or two (symmetric dendrimers, $(\mathbf{D}n)_2\mathbf{B}^{2+}$) first-, second-, or third-generation 1,3-dimethyleneoxybenzene (Fréchet-type) dendrons appended. Association is thermodynamically driven by electron donor−acceptor interactions.

The assembling process has been investigated by NMR and UV/vis absorption and fluorescence spectroscopy and electrochemical measurements. We have measured the association constants, demonstrated that the assembling/disassembling process can be controlled by redox stimulation, and obtained some interesting information on the structure of the host−guest species and the dynamics of their formation.

Results and Discussion

Photophysical and Electrochemical Properties of Tweezer T. The absorption and emission spectra of tweezer **T** in dichloromethane solution are shown in Figure 2. The relatively weak, low-energy absorption bands are typical of the naphthalene chromophoric group.[47] The strong fluorescence band with $\lambda_{max} = 344$ nm, $\tau = 9.5$ ns, and $\Phi = 0.53$ can also be assigned to the naphthalene unit.

In dichloromethane/acetonitrile (9:1) solution, tweezer **T** shows an irreversible oxidative process at +1.6 V, whereas no reduction process has been observed in the potential window of the solvent used (up to −2.0 V vs SCE).

Photophysical Properties of Symmetric and Unsymmetric Dendrimers. The investigated dendrimers contain three types of chromophoric groups, namely 4,4′-bipyridinium, 1,3-dimethyleneoxybenzene, and benzene. The ratios among these three types of groups are different in each dendrimer: the two limiting cases are 1:1:1 for $\mathbf{D}1\mathbf{B}^{2+}$ and 1:14:16 for $(\mathbf{D}3)_2\mathbf{B}^{2+}$. The 4,4′-

(6) (a) Xu, M.-H.; Lin, J.; Hu, Q.-S.; Pu, L. *J. Am. Chem. Soc.* **2002**, *124*, 14239. (b) Pugh, V. J.; Hu, Q. S.; Zuo, X.; Lewis, F. D.; Pu, L. *J. Org. Chem.* **2001**, *66*, 6136. (c) Balzani, V.; Ceroni, P.; Gestermann, S.; Kauffmann, C.; Gorka, M.; Vögtle, F. *Chem. Commun.* **2000**, 853.
(7) (a) Vicinelli, V.; Ceroni, P.; Maestri, M.; Balzani, V.; Gorka, M.; Vögtle, F. *J. Am. Chem. Soc.* **2002**, *124*, 6461. (b) Serin, J. M.; Brousmiche, D. W.; Fréchet, J. M. J. *J. Am. Chem. Soc.* **2002**, *124*, 11848.
(8) (a) Dichel, W. R.; Serin, J. M.; Edder, C.; Fréchet, J. M. J.; Matuszewski, M.; Tan, L.-S.; Ohulchanskyy, T. Y.; Prasad, P. N. *J. Am. Chem. Soc.* **2004**, *126*, 5380. (b) Hecht, S.; Frèchet, J. M. J. *J. Am. Chem. Soc.* **2001**, *123*, 6959.
(9) (a) Daniel, M.-C.; Ruiz, J.; Astruc, D. *Inorg. Chem.* **2004**, *43*, 8649. (b) Daniel, M.-C.; Ruiz, J.; Blais, J.-C.; Daro, N.; Astruc, D. *Chem. Eur. J.* **2003**, *9*, 4371. (c) Daniel, M.-C.; Ruiz, J.; Astruc, D. *J. Am. Chem. Soc.* **2003**, *125*, 1150.
(10) Kim, E.; Kim, K.; Yang, H.; Kim, Y. T.; Kwak, J. *Anal. Chem.* **2003**, *75*, 5665.
(11) (a) Ruiz, J.; Pradet, C.; Varret, F.; Astruc, D. *Chem. Commun.* **2002**, 1108. (b) Nlate, S.; Ruiz, J.; Sartor, V.; Navarro, R.; Blais, J.-C.; Astruc, D. *Chem. Eur. J.* **2000**, *6*, 2544.
(12) (a) Gorman, C. B.; Smith, J. C. *Acc. Chem. Res.* **2001**, *34*, 60. (b) Cardona, C. M.; Mendoza, S.; Kaifer, A. E. *Chem. Soc. Rev.* **2000**, *29*, 37.
(13) See, e.g.: (a) Chasse, T. L.; Gorman, C. B. *Langmuir* **2004**, *20*, 8792. (b) Marchioni, F.; Venturi, M.; Credi, A.; Balzani, V.; Belohradsky, M.; Elizarov, A. M.; Tseng, H.-R.; Stoddart, J. F. *J. Am. Chem. Soc.* **2004**, *126*, 568. (c) McClenahan, N. D.; Passalacqua, R.; Loiseau, F.; Campagna, S.; Verheyde, B.; Hameurlaine, A.; Dehaen, W. *J. Am. Chem. Soc.* **2003**, *125*, 5356. (d) Rio, Y.; Accorsi, G.; Armaroli, N.; Felder, D.; Levillain, E.; Nierengarten, J.-F. *Chem. Commun.* **2002**, 2830.
(14) See, e.g.: (a) Cross, J. P.; Lauz, M.; Badger, P. D.; Petoud, S. *J. Am. Chem. Soc.* **2004**, *126*, 16278. (b) Nakajima, R.; Tsuruta, M.; Higuchi, M.; Yamamoto, K. *J. Am. Chem. Soc.* **2004**, *126*, 1630. (c) Vögtle, F.; Gorka, M.; Vicinelli, V.; Ceroni, P.; Maestri, M.; Balzani, V. *ChemPhysChem* **2001**, *12*, 769. (d) Zhou, L.; Russell, D. H.; Zhao, M.; Crooks, R. M. *Macromolecules* **2001**, *34*, 3567.
(15) See e.g.: (a) Broeren, M. A. C.; van Dongen, J. L. J.; Pittelkow, M.; Chrisensen, J. B.; van Genderen, M. H. P.; Meijer, E. W. *Angew. Chem., Int. Ed.* **2004**, *43*, 3557. (b) Yamaguchi, T.; Ishii, N.; Tashiro, K.; Aida, T. *J. Am. Chem. Soc.* **2003**, *125*, 13934. (c) Morgan, M. T.; Carnahan, M. A.; Immoos, C. E.; Ribeiro, A. A.; Finkelstein, S.; Lee, S. J.; Grinstaff, M. W. *J. Am. Chem. Soc.* **2003**, *125*, 15485. (d) Balzani, V.; Ceroni, P.; Gestermann, S.; Gorka, M.; Kauffmann, C.; Vögtle, F. *Tetrahedron* **2002**, *58*, 629. (e) Dykes, G. M.; Brierley, L. J.; Smith, D. K.; McGrail, P. T.; Seeley, G. *Chem. Eur. J.* **2001**, *7*, 4730.
(16) Diederich, F.; Felber, B. *Proc. Natl. Acad. Sci. U.S.A.* **2002**, *99*, 4778.
(17) (a) Bergamini, G.; Ceroni, P.; Balzani, V.; Cornelissen, L.; van Heyst, J.; Lee, S.-K.; Vögtle, F. *J. Mater. Chem.* **2005**, *15*, 2959. (b) Saudan, C.; Ceroni, P.; Vicinelli, V.; Maestri, M.; Balzani, V.; Gorka, M.; Lee, S.-K.; van Heyst, J.; Vögtle, F. *Dalton Trans.* **2004**, 1597. (c) Bergamini, G.; Saudan, C.; Ceroni, P.; Maestri, M.; Balzani, V.; Gorka, M.; Lee, S.-K.; van Heyst, J.; Vögtle, F. *J. Am. Chem. Soc.* **2004**, *126*, 16466. (d) Saudan, C.; Balzani, V.; Gorka, M.; Lee, S.-K.; van Heyst, J.; Maestri, M.; Ceroni, P.; Vicinelli, V.; Vögtle, F. *Chem. Eur. J.* **2004**, *10*, 899. (e) Saudan, C.; Balzani, V.; Gorka, M.; Lee, S.-K.; Maestri, M.; Vicinelli, V.; Vögtle, F. *J. Am. Chem. Soc.* **2003**, *125*, 4424. (f) Enoki, O.; Imaoka, T.; Yamamoto, K. *Org. Lett.* **2003**, *5*, 2547.
(18) Ong, W.; Gómez-Kaifer, M.; Kaifer, A. E. *Chem. Commun.* **2004**, 1677.
(19) Gibson, H. W.; Yamaguchi, N.; Hamilton, L.; Jones, J. W. *J. Am. Chem. Soc.* **2002**, *124*, 4653.
(20) van Bommel, K. J. C.; Metselaar, G. A.; Verboom, W.; Reinhoudt, D. N. *J. Org. Chem.* **2001**, *66*, 5405.
(21) Lee, J. W.; Ko, Y. H.; Park, S.-H.; Yamaguchi, K.; Kim, K. *Angew. Chem., Int. Ed.* **2001**, *40*, 746.
(22) (a) Ong, W.; Grindstaff, J.; Sobransingh, D.; Toba, R.; Quintela, J. M.; Peinador, C.; Kaifer, A. E. *J. Am. Chem. Soc.* **2005**, *127*, 3353. (b) Moon, M.; Grindstaff, J.; Sobransingh, D.; Kaifer, A. E. *Angew. Chem., Int. Ed.* **2004**, *43*, 5496. (c) Ong, W.; Kaifer, A. E. *Angew. Chem., Int. Ed.* **2003**, *42*, 2164. (d) Toba, R.; Quintela, J. M.; Peinador, C.; Román, E.; Kaifer, A. E. *Chem. Commun.* **2002**, 1768. (e) Ong, W.; Kaiser, A. E. *J. Am. Chem. Soc.* **2002**, *124*, 9358. (f) Cardona, C. M.; McCarley, T. D.; Kaifer, A. E. *J. Org. Chem.* **2000**, *65*, 1857.
(23) Balzani, V.; Ceroni, P.; Giansante, C.; Vicinelli, V.; Klärner, F.-G.; Verhaelen, C.; Vögtle, F.; Hahn, U. *Angew. Chem., Int. Ed.* **2005**, *44*, 4574.
(24) For a somewhat related gas-phase study of these systems, see: Schalley, C. A.; Verhaelen, C.; Klärner, F.-G.; Hahn, U.; Vögtle, F. *Angew. Chem., Int. Ed.* **2005**, *44*, 477.
(25) (a) Klärner, F.-G.; Kahlert, B. *Acc. Chem. Res.* **2003**, *36*, 919. (b) Marchioni, F.; Juris, A.; Lobert, M.; Seelbach, U. P.; Kahlert, B.; Klärner, F.-G. *New J. Chem.* **2005**, *29*, 780.

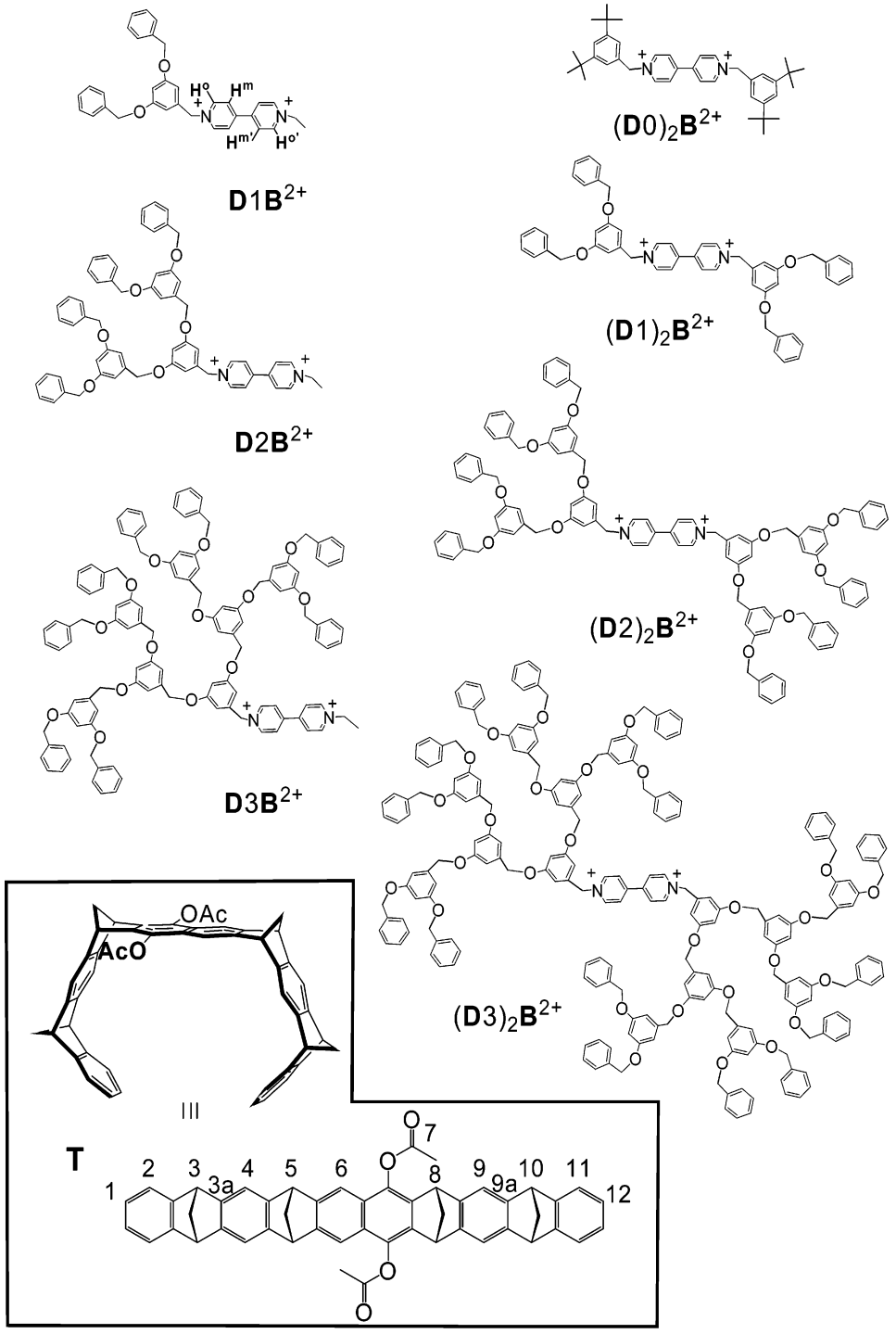

Figure 1. Formulas of the investigated compounds: **D** stands for dendron, *n* indicates the dendron generation ($n = 1, 2, 3$), and $\mathbf{B}^{2+}$ stands for the 4,4′-bipyridinium core.

bipyridinium species exhibit a strong absorption band around 260 nm (for 4,4′-dimethylbipyridinium, $\lambda_{max} = 259$ nm, $\epsilon = 20\,700$ M^{-1} cm^{-1}; for 4,4′-dibenzylbipyridinium, $\lambda_{max} = 259$ nm, $\epsilon = 22\,700$ M^{-1} cm^{-1}), while 1,3-dimethyleneoxybenzene shows a relatively weak absorption band around 275 nm ($\epsilon = 2200$ M^{-1} cm^{-1})[26] and benzene a very weak band at 255 nm ($\epsilon = 250$ M^{-1} cm^{-1}).[47] As previously reported for the symmetric $(\mathbf{D}n)_2\mathbf{B}^{2+}$ dendrimers,[27] the absorption spectra of the unsymmetric ones (see, e.g., $\mathbf{D}1\mathbf{B}^{2+}$ in Figure 3) do not coincide with the summation of the spectra of the component units, particularly because of the presence of a broad and weak absorption tail above 300 nm that is assigned to a charge-transfer (CT) transition from 1,3-dimethyleneoxybenzene electron-donor units to the 4,4′-bipyridinium electron-acceptor core. The inset of Figure 3 shows the variation of the molar absorption coefficients at 280 nm, where only 4,4′-bipyridinium and 1,3-dimethyleneoxybenzene absorb, versus the number *n* of 1,3-dimethyleneoxybenzene units. The linear fit is not fully satisfactory,

(26) The value of the molar absorption coefficient for the dimethoxybenzene unit was obtained from the absorption spectrum of dendron **D**2 (Figure 2).

(27) Ceroni, P.; Vicinelli, V.; Maestri, M.; Balzani, V.; Müller, W. M.; Müller, U.; Hahn, U.; Osswald, F.; Vögtle, F. *New J. Chem.* **2001**, *25*, 989.

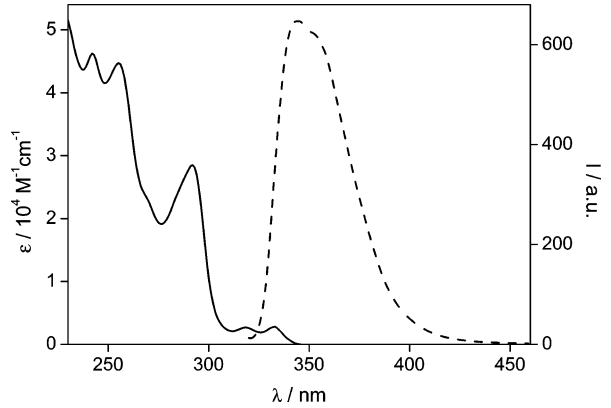

Figure 2. Absorption (solid line) and emission (dashed line) spectra of an air-equilibrated dichloromethane solution of the tweezer **T** at room temperature.

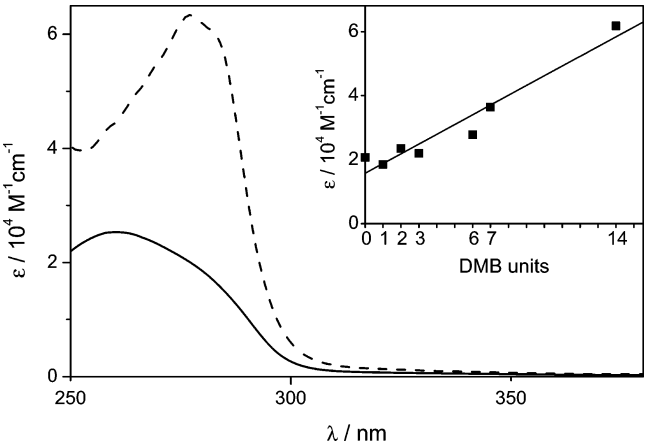

Figure 3. Absorption spectra of $\mathbf{D}1\mathbf{B}^{2+}$ (solid line) and of $(\mathbf{D}3)_2\mathbf{B}^{2+}$ (dashed line) in air-equilibrated acetonitrile/dichloromethane (1:1 v/v) solution at room temperature. Inset shows molar absorption coefficients of the dendrimers at 280 nm versus the number (n) of dimethyleneoxybenzene units. For DMB units = 0, the ϵ value for 4,4′-dimethylbypiridinium is reported.

likely because of the above-mentioned CT interactions among the chromophoric units in both the symmetric and unsymmetric dendrimers.

Dimethyleneoxybenzenes[47] and, accordingly, Fréchet-type dendrons[28] are known to exhibit fluorescence ($\lambda_{max} = 350$ nm and $\tau < 1$ ns). Such a band is no longer present in both the symmetric[27] and unsymmetric dendrimers. This result shows that the fluorescent excited state of the 1,3-dimethyleneoxybenzene units ($E_{00} \approx 4.1$ eV) is quenched by the 4,4′-bipyridinium core via a fast electron-transfer process, as expected from the negative free energy change ($\Delta G \approx -2$ eV).[29]

Electrochemical Properties of Symmetric and Unsymmetric Dendrimers. The investigated dendrimers contain the well-known[30] 4,4′-bipyridinium electroactive unit, $\mathbf{B}^{2+}$. Such a unit undergoes two successive, reversible, one-electron reduction processes at easily accessible potentials that correspond to the formation of a cation radical ($\mathbf{B}^{2+} \rightarrow \mathbf{B}^{+}$) and a neutral ($\mathbf{B}^{+} \rightarrow \mathbf{B}$) species. The monoreduced species $\mathbf{B}^{+}$ shows a characteristic, very strong absorption in the visible region. Because of their electron-acceptor properties, 4,4′-bipyridinium species can

Table 1. Half-Wave Potentials (V vs SCE) in Dichloromethane/Acetonitrile (9:1 v/v), $[NBu_4]PF_6$ 0.1 M, unless Otherwise Noted

	$\mathbf{B}^{2+} \rightarrow \mathbf{B}^{+}$	$\mathbf{B}^{+} \rightarrow \mathbf{B}$
$\mathbf{D}1\mathbf{B}^{2+}$	−0.29	−0.77
$\mathbf{D}1\mathbf{B}^{2+}\cdot\mathbf{T}^{b}$	−0.36	−0.77
$\mathbf{D}2\mathbf{B}^{2+}$	−0.27	−0.73
$\mathbf{D}2\mathbf{B}^{2+}\cdot\mathbf{T}^{b}$	−0.33	−0.73
$\mathbf{D}3\mathbf{B}^{2+}$	−0.27	−0.73
$\mathbf{D}3\mathbf{B}^{2+}\cdot\mathbf{T}^{b}$	−0.33	−0.73
$(\mathbf{D}1)_2\mathbf{B}^{2+\,a}$	−0.25	−0.73
$(\mathbf{D}1)_2\mathbf{B}^{2+}\cdot\mathbf{T}^{a,b}$	−0.30	−0.73
$(\mathbf{D}2)_2\mathbf{B}^{2+}$	−0.24	−0.72
$(\mathbf{D}2)_2\mathbf{B}^{2+}\cdot\mathbf{T}^{b}$	−0.31	−0.72
$(\mathbf{D}3)_2\mathbf{B}^{2+}$	−0.24	−0.72
$(\mathbf{D}3)_2\mathbf{B}^{2+}\cdot\mathbf{T}^{b}$	−0.30	−0.72

[a] Dichloromethane/acetonitrile (3:1 v/v). [b] Under the experimental conditions used, more than 95% of the electroactive species is in the complexed form.

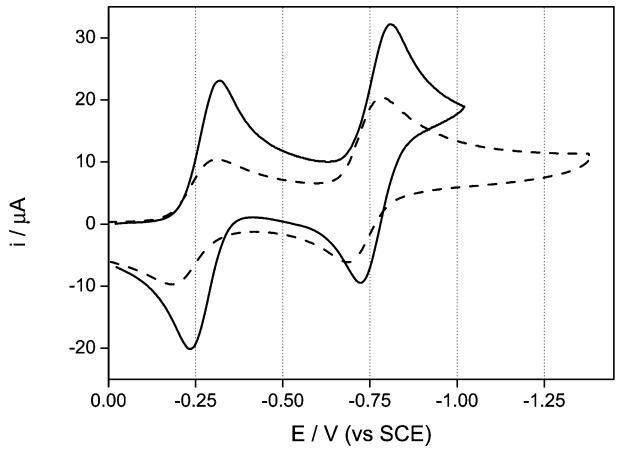

Figure 4. Cyclic voltammetric curves for $\mathbf{D}1\mathbf{B}^{2+}$ (solid line) and $(\mathbf{D}3)_2\mathbf{B}^{2+}$ (dashed line), 1.1 mM in acetonitrile/dichloromethane (1:9 v/v)−$[NBu_4]PF_6$ (0.1 M) solution. Scan rate $\upsilon = 0.2$ V/s.

interact with electron-donor compounds to form adducts in a variety of structures, including pseudorotaxanes, rotaxanes, and catenanes.[31]

In agreement with these expectations, the $\mathbf{D}n\mathbf{B}^{2+}$ unsymmetric dendrimers, as well as the $(\mathbf{D}n)_2\mathbf{B}^{2+}$ symmetric ones,[32] show two reversible one-electron-transfer processes. The half-wave potential values ($E_{1/2}$) observed for reduction of the six dendrimers are gathered in Table 1. The cyclic voltammetric (CV) curves recorded, under the same experimental conditions, for equimolar solutions of $\mathbf{D}1\mathbf{B}^{2+}$ and $(\mathbf{D}3)_2\mathbf{B}^{2+}$ are shown in Figure 4; the higher current intensities for $\mathbf{D}1\mathbf{B}^{2+}$ compared to those for $(\mathbf{D}3)_2\mathbf{B}^{2+}$ reflect its higher diffusion coefficient, as expected on the basis of the lower molecular mass. With regard to the $E_{1/2}$ values, the diagram of Figure 5 shows that (i) reduction potentials are slightly negatively shifted (30−40 mV) for the unsymmetric compared to the symmetric ones and (ii) within each family, the first-generation dendrimer shows a slight negative shift of both reduction processes compared to the second- and third-generation ones.[33] The $E_{1/2}$ values reported

(28) Stewart, G. M.; Fox, M. A. *J. Am. Chem. Soc.* **1996**, *118*, 4354.
(29) Balzani, V.; Scandola, F. *Supramolecular photochemistry*; Ellis Horwood: Chichester, England, 1991.
(30) Monk, P. M. S.; *The Viologens: physicochemical properties, synthesis, and applications of the salts of 4,4′-bipyridine*; Wiley: New York, 1998.
(31) Balzani, V.; Credi, A.; Raymo, F. M.; Stoddart, J. F. *Angew. Chem., Int. Ed.* **2000**, *39*, 3348.
(32) Toba, R.; Quintela, J. M.; Peinador, C.; Román, E.; Kaifer, A. E. *Chem. Commun.* **2001**, 857.
(33) Kaifer et al.[22a] reported a very small positive shift of the first reduction process in acetonitrile solution upon increasing the generation from 1 to 3 in a series of dendrimers differing from the present $\mathbf{D}n\mathbf{B}^{2+}$ one in the substituent at the apical position of the bipyridinium residue.

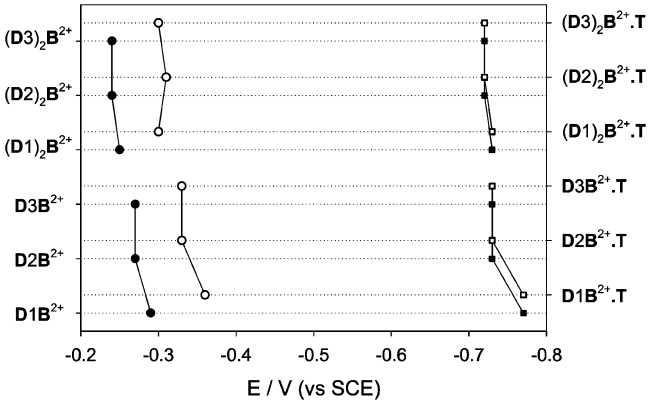

Figure 5. Half-wave potentials for the reduction processes of the symmetric and unsymmetric dendrimers and for their adducts with **T**.

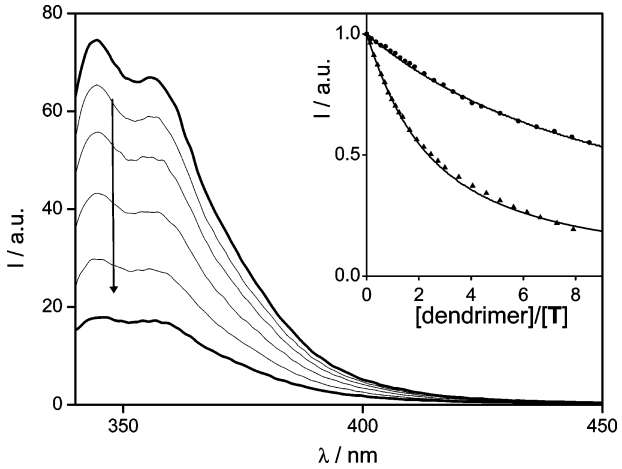

Figure 6. Changes in the fluorescence spectra of a 1.6×10^{-5} M solution of **T** upon titration with $(\mathbf{D}3)_2\mathbf{B}^{2+}$. Experimental conditions: dichloromethane solution, room temperature, excitation at 334 nm. The inset shows the titration curve obtained by plotting the emission intensity at 356 nm as a function of the equivalents of $\mathbf{D}1\mathbf{B}^{2+}$ (triangles) and of $(\mathbf{D}3)_2\mathbf{B}^{2+}$ (circles). The points have been corrected for the fraction of light absorbed by **T**. The solid line shows the fitting based on formation of a 1:1 complex.

in Table 1 show that the 4,4′-bipyridinium core is easily accessible to the electrode surface and slightly affected by the presence of the dendritic branches.

The rate of electron transfer to the electrode surface is high for all the dendrimers (see Figure 4). For example, in the case of $(\mathbf{D}3)_2\mathbf{B}^{2+}$, the two reduction processes show a Nernstian behavior at scan rates up to 5 V/s, thus indicating no significant inhibition or site isolation effect on the dendrimer core by the dendrons.

Host−Guest Formation from Fluorescence and Electrochemical Measurements. As mentioned above, the tweezer **T** exhibits a strong fluorescence band with $\lambda_{max} = 344$ nm. When a ca. 10^{-5} M air-equilibrated dichloromethane solution of **T** was titrated with each of the dendrimers, small changes were observed in the absorption spectrum of the solution with respect to the mere summation of the two components spectra. On the other hand, the fluorescence band of the tweezer was strongly (but not completely, vide infra) quenched, as shown in Figure 6 for the case of $(\mathbf{D}3)_2\mathbf{B}^{2+}$. Since dynamic quenching can be ruled out because of the short (9.5 ns) excited-state lifetime of **T**, these results indicate that tweezer and dendrimers give rise to adducts. We have also verified that the fluorescence of **T** is not quenched upon addition to the solution of the dendrons used

Table 2. Association Constants, K_a, of the Complexes between Tweezer **T** and Various Bipyridinium Salts

bipyridinium salt	K_a ($\times 10^3$ M^{-1})	
$\mathbf{D}1\mathbf{B}^{2+}$	34[a]	29[b]
		1.5[c]
$\mathbf{D}2\mathbf{B}^{2+}$	22[a]	16[b]
$\mathbf{D}3\mathbf{B}^{2+}$	16[a]	
$(\mathbf{D}0)_2\mathbf{B}^{2+}$		8.4[b,e]
		0.7[d,e]
$(\mathbf{D}1)_2\mathbf{B}^{2+}$	27[a,e]	
		1.6[c]
$(\mathbf{D}2)_2\mathbf{B}^{2+}$	18[a,e]	
$(\mathbf{D}3)_2\mathbf{B}^{2+}$	9[a,e]	

[a] Spectrofluorimetric titration in CH_2Cl_2 at room temperature. Experimental error, 10%. [b] ^{1}H NMR titration at 25 °C, experimental error ≤20% in CD_2Cl_2. [c] As above in CD_2Cl_2/acetone-d_6 (1:2). [d] As above in $CDCl_3$/acetone-d_6 (1:2). [e] Reported in ref 23.

to build up the dendrimers. Therefore, we conclude that adduct formation must involve an interaction between the tweezer and the bipyridinium dendritic cores. This conclusion was fully confirmed by electrochemical experiments. We found that the CV pattern for reduction of the dendritic cores is affected by the addition of tweezer. In particular, both the cathodic and anodic peaks corresponding to the first one-electron reduction process of a dendritic core progressively move to more negative values upon addition of tweezer, whereas the peaks corresponding to the second reduction process were practically unaffected (see Table 1 and Figure 5).

To elucidate the stoichiometry and the strength of adduct formation (Table 2), we performed fluorescence titration experiments, taking into account[34] the fraction of light absorbed by the dendrimer. The titration plot obtained for 1.6×10^{-5} M solutions of **T** upon addition of $\mathbf{D}1\mathbf{B}^{2+}$ and $(\mathbf{D}3)_2\mathbf{B}^{2+}$ are shown in the inset of Figure 6.

From a qualitative viewpoint, the behavior of the titration plots (see, e.g., inset to Figure 6) could be interpreted in two different ways: (i) If the fluorescence intensity of the tweezer molecules involved in adduct formation is completely quenched, the results indicate that a significant fraction of tweezer molecules remain free. (ii) If all the tweezer molecule are involved in adduct formation, in such an adduct the fluorescence intensity of the tweezer is only partly quenched. This problem can be solved by measuring the fluorescence lifetime of the tweezer in the absence and in the presence of dendrimers. In case (i), the fluorescence lifetime should be the same; in case (ii), the fluorescence lifetime should decrease by a factor comparable to that of emission intensity quenching. We have found that the lifetime of the tweezer fluorescence is 9.5 ns both in the absence and in the presence of dendrimers (up to 10 equiv) and that there is no evidence of a double exponential decay. Therefore, we conclude that the complexed species do not show any appreciable fluorescence and that, even after addition of an excess of dendrimer, a significant fraction of tweezer molecules remain uncomplexed.

NMR Investigation. (a) Association Constants. The conclusions drawn from the spectrofluorimetric titration experiments were fully confirmed by NMR investigations. The complex formation between tweezer **T** and 4,4′-bipyridinium guest molecules could be detected by the characteristic upfield shifts

(34) Credi, A.; Prodi, L. *Spectrochim. Acta A* **1998**, *54*, 159.

Table 3. Complexation-Induced ^{1}H NMR Shifts of the Bipyridinium Guest Protons at 25 °C

complex	H^o	$H^{o'}$	H^m	$H^{m'}$	$N^+–CH_2$	$N^+–CH_2CH_3$
$\mathbf{D}1\mathbf{B}^{2+}\cdot\mathbf{T}$	0.79[a]	2.93[a]	2.41[a]	3.19[a]	0.19[a]	1.23[a]
	1.47[d]	1.60[d]	2.99[d]	3.59[d]	0.29[d]	0.51[d]
	0.4[b]	0.35[b]	0.8[b]	0.8[b]	0.06[b]	0.09[b]
$\mathbf{D}2\mathbf{B}^{2+}\cdot\mathbf{T}$	0.61[a]	–[c]	–[c]	–[c]	0.13[a]	0.72[a]
	0.4[b]	0.52[b]	1.0[b]	1.0[b]	0.09[b]	0.08[b]
$(\mathbf{D}1)_2\mathbf{B}^{2+}\cdot\mathbf{T}$	1.35[d]		–[c]		0.28[d]	
$(\mathbf{D}0)_2\mathbf{B}^{2+}\cdot\mathbf{T}$	0.91[a]		3.22[a]		0.17[a]	

[a] $\Delta\delta_{max}$ in CD_2Cl_2. [b] $\Delta\delta_{obs}$ in acetone-d_6 with $[\mathbf{T}] = 7.1 \times 10^{-4}$ M and $[\mathbf{D}1\mathbf{B}^{2+}] = 7.4 \times 10^{-4}$ M or $[\mathbf{D}2\mathbf{B}^{2+}] = 7.6 \times 10^{-4}$ M. [c] Not detectable because of the signal broadening. [d] $\Delta\delta_{max}$ in CD_2Cl_2/acetone-d_6 (1:2).

of the ^{1}H NMR signals of the guest protons. The maximum complexation-induced ^{1}H NMR shifts, $\Delta\delta_{max}$, the association constants, K_a, and hence the Gibbs energies of association, ΔG_{ass}, were determined for the formation of the complexes of tweezer **T** with the unsymmetric dendrimers of first- and second-generation $\mathbf{D}n\mathbf{B}^{2+}$ ($n = 1, 2$) and the symmetric dendrimers $(\mathbf{D}0)_2\mathbf{B}^{2+}$ and $(\mathbf{D}1)_2\mathbf{B}^{2+}$ by the use of ^{1}H NMR titrations (Tables 2 and 3). In the other cases, the signals of the dendrimer protons in the presence of tweezer **T** are very broad and could not be assigned. In addition to the thermodynamic parameters, the stoichiometry was determined through Job plot analysis to be 1:1 for the complex between **T** and $(\mathbf{D}0)_2\mathbf{B}^{2+}$.

The binding constants, K_a, obtained by ^{1}H NMR titrations are in good agreement with those determined by spectrofluorimetric measurements (Table 2). In dichloromethane solution, tweezer **T** forms highly stable complexes with the symmetric and unsymmetric dendrimers, with values of the binding constants in the order of 10^4 M^{-1} which decrease with increasing dendrimer generation. The complexes of the unsymmetric dendrimers are more stable than those of the corresponding symmetric dendrimers of the same generation. A similar dependence of the complex stability on the size of the dendrimer was observed in the gas phase by mass spectroscopy.[24] Apparently, even in solution (but only in a nonpolar solvent), the bipyridinium core is stabilized by "intramolecular solvation", which results from the back-folding of the electron-donor branches, an effect that increases with increasing dendrimer generation. In acetone, the complex stabilities are much lower than in dichloromethane, indicating that the bipyridinium dication is substantially stabilized by solvation with the polar solvent.

(b) Kinetic Measurements. The large $\Delta\delta_{max}$ values observed for the protons at the bipyridinium core in the complexes of the dendrimers with tweezer **T** and the temperature dependence of the ^{1}H NMR spectra (vide infra) provide good evidence that one of the pyridinium rings is positioned inside and the other one outside the cavity of the tweezer **T** and that **T** shuttles from one pyridinium ring to the other. At room temperature, the shuttling as well as the complex dissociation/association processes are fast and lead to an averaging of the ^{1}H NMR signals of the free and complexed guest and host protons.

The kinetics of the dissociation/association process could be analyzed on the basis of the temperature dependence of the ^{1}H NMR spectra of 2:1 mixtures of tweezer **T** with $(\mathbf{D}0)_2\mathbf{B}^{2+}$, $(\mathbf{D}1)_2\mathbf{B}^{2+}$, or $\mathbf{D}1\mathbf{B}^{2+}$. In the ^{1}H NMR spectrum of a 2:1 mixture of **T** and $(\mathbf{D}0)_2\mathbf{B}^{2+}$ dissolved in $CDCl_3$/acetone-d_6 (1:2) (Figure 7), the four ^{1}H NMR signals (assigned to the bridgehead protons of **T**) are broadened upon lowering the temperature, and finally

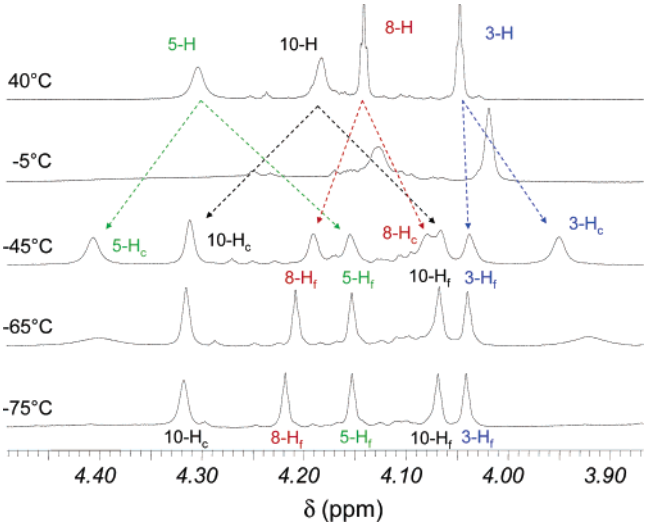

Figure 7. ^{1}H NMR spectra of a 2:1 mixture of **T** and $(\mathbf{D}0)_2\mathbf{B}^{2+}$ in $CDCl_3$/acetone-d_6 (1:2) at various temperatures. In the spectrum at −45 °C, the ^{1}H NMR signals at $\delta = 4.191$, 4.155, 4.066, and 4.038 ppm could be assigned to protons 8-H_f, 5-H_f, 10-H_f, and 3-H_f of the free tweezer by comparison with the ^{1}H NMR spectrum of **T**. The ^{1}H NMR signals at $\delta = 4.407$, 4.312, 4.079, and 3.950 were assigned to the corresponding protons 5-H_c, 10-H_c, 8-H_c, and 3-H_c of complex $(\mathbf{D}0)_2\mathbf{B}^{2+}\cdot\mathbf{T}$ by 2D NMR experiments. At temperatures lower than −45 °C, the signals assigned to 3-H_c, 5-H_c, and 8-H_c of the complex are broadened and coalesce at −75 °C because of "freezing" out the shuttling process. The signal assigned to 10-H_c remains sharp at lower temperatures apparently due to an accidental equivalence of 10-H_c (in) and 10-H_c (out) in the frozen complex $(\mathbf{D}0)_2\mathbf{B}^{2+}\cdot\mathbf{T}$ (see Figure 11).

at −45 °C each signal is split into two signals which could be assigned to free and complexed **T** by comparison with the ^{1}H NMR spectrum of isolated **T** and by HH−COSY 2D NMR experiments. The specific rate constants of the exchange between free and complexed tweezer **T** were determined from the line-shape analysis of the temperature-dependent signals assigned to the bridgehead protons 5-H and 10-H, which show the largest splitting at low temperature. The temperature dependence of the rate constants allows us to calculate the activation parameters of the exchange between complexed and free tweezer, which are a measure for the dissociation parameters (Figure 8).[35] Similar temperature-dependent NMR spectra were observed for the 2:1 mixture of **T** and $(\mathbf{D}1)_2\mathbf{B}^{2+}$ dissolved in CD_2Cl_2/acetone-d_6 (1:2) (Figure 9). In this case, only the line shapes of the temperature-dependent signals assigned to 5-H could be analyzed because of the partial overlap of the other signals at −55 °C (in the range of slow exchange). Although the exchange between complexed and free tweezer is again slow in the ^{1}H NMR spectrum of the 2:1 mixture of **T** and $\mathbf{D}1\mathbf{B}^{2+}$ dissolved in CD_2Cl_2/acetone-d_6 (1:2) at −75 °C, no line-shape analysis could be performed because the signals of the tweezer bridgehead protons show a stronger overlap at low temperature than the corresponding signals in the other spectra discussed above. In this case the specific rate constant, k, and hence the Gibbs energy of activation, $\Delta G^{\ddagger}$, could be estimated from the

(35) Two processes—the dissociation/association and a less likely S_N2-like transfer of the guest molecule from the complex to the empty tweezer—have to be taken into consideration for the observed exchange. Therefore, the observed activation enthalpy is either equal to or smaller than the dissociation enthalpy. The dynamics in the host−guest complexes are discussed in more detail for the complexes between tweezer **T** and 1,2,4,5-tetracyanobenzene or tropylium tetrafluoroborate as examples: Lobert, M.; Bandmann, H.; Burkert, U.; Büchele, U. P.; Podsadlowski, V.; Klärner, F.-G. *Chem. Eur. J.*, in press.

$(D0)_2B^{2+}$•T				$(D1)_2B^{2+}$•T	
	5-H	10-H	Average [(a)]		5-H [(b)]
T [°C]	k [s^{-1}]	k [s^{-1}]	k [s^{-1}]	T [°C]	k [s^{-1}]
25	2200	1900	2050	25	3000
10	800	800	800	10	1300
- 5	240	240	240	- 5	570
- 25	50	50	50	-15	310
- 45	12	12	12	-25	190
				-35	76
				-45	40
				- 55	24

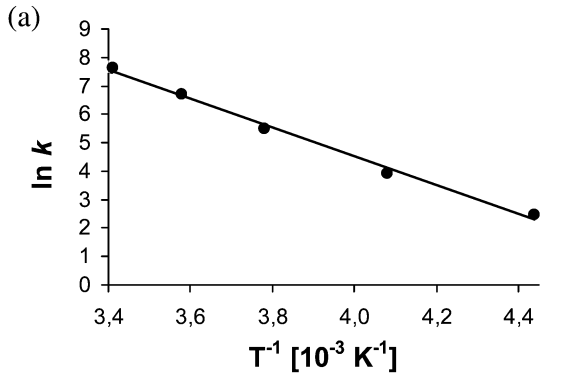

A [s^{-1}]	$4.23 \cdot 10^{+10}$
E_a [kcal • mol^{-1}]	(10.04 ± 0.44)
T_m [K]	263.00
r^2	0.9942
$\Delta H^{\neq}$ [kcal • mol^{-1}]	(9.51 ± 0.44)
$\Delta G^{\neq}$ [kcal • mol^{-1}]	(12.58 ± 0.63)
$\Delta S^{\neq}$ [cal • mol^{-1} • K^{-1}]	- (11.65 ± 1.70)

A [s^{-1}]	$1.74 \cdot 10^{+9}$
E_a [kcal • mol^{-1}]	(7.9 ± 0.2)
T_m [K]	258.00
r^2	0.9946
$\Delta H^{\neq}$ [kcal • mol^{-1}]	(7.4 ± 0.2)
$\Delta G^{\neq}$ [kcal • mol^{-1}]	(12.0 ± 0.3)
$\Delta S^{\neq}$ [cal • mol^{-1} • K^{-1}]	- (18.0 ± 0.9)

Figure 8. Determination of the activation parameters (free energy of activation, $\Delta G^{\ddagger}$, enthalpy of activation, $\Delta H^{\ddagger}$, and entropy of activation, $\Delta S^{\ddagger}$) from the temperature dependence of the specific rate constants k of the dissociation of complex $(\mathbf{D}0)_2\mathbf{B}^{2+}\cdot\mathbf{T}$ and $(\mathbf{D}1)_2\mathbf{B}^{2+}\cdot\mathbf{T}$ in $CDCl_3$/acetone-d_6 (1:2) and CD_2Cl_2/acetone-d_6 (1:2), respectively.

difference in the resonance frequencies, $\delta\nu = \nu(5\text{-}H_c) - \nu(5\text{-}H_f) = 57.5$ Hz, to be $k = 2.22\ \delta\nu = 127.7\ s^{-1}$ and $\Delta G^{\ddagger} = 10.5$ kcal mol^{-1} at the temperature of coalescence (−55 °C).[36] Similar results were obtained for the complex formation between **T** and $(\mathbf{D}0)_2\mathbf{B}^{2+}$ dissolved in pure CD_2Cl_2. Due to the partial overlap of the signals of the bridgehead protons of free and complexed tweezer, only the specific rate constant and the Gibbs activation energy could be estimated here to be $k = 2.22\ \delta\nu = 222\ s^{-1}$ and $\Delta G^{\ddagger} = 13.0$ kcal mol^{-1} at the temperature of coalescence (0 °C).

(36) Günther, H. *NMR−Spektroskopie*; 1. Auflage, Georg Thieme Verlag: Stuttgart, 1973; S. 248.

Beside dissociation/association, two "intramolecular" dynamic processes have to be considered to explain the ^{1}H NMR spectra of the complexes at low temperature: (i) the already mentioned shuttling process and (ii) the guest rotation inside the tweezer cavity around the long axis of the bipyridinium core. The shuttling process leads to an averaging of the protons $H^o/H^{o'}$ and $H^m/H^{m'}$ at the bipyridinium unit, which are nonequivalent even in the complexes of the symmetric dendrimers $(\mathbf{D}n)_2\mathbf{B}^{2+}$ ($n = 0-3$), and the rotation causes the averaging of the protons H^o/H^o and H^m/H^m or $H^{o'}/H^{o'}$ and $H^{m'}/H^{m'}$ at one and the same pyridinium ring, which are nonequivalent in the complexes due to the acetoxy substituents at the central naphthalene spacer unit

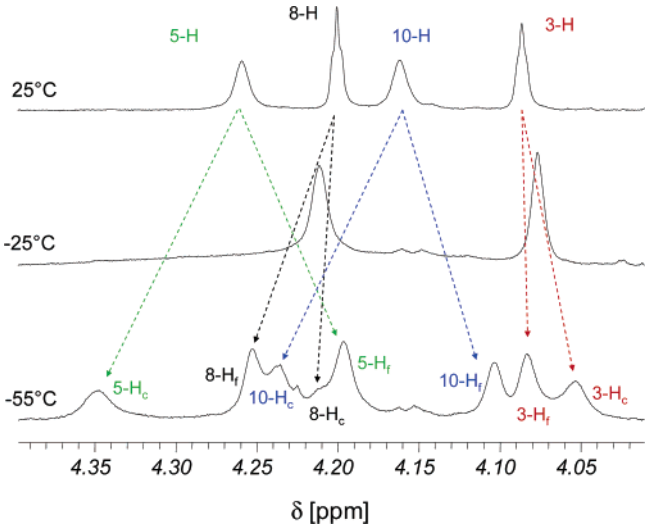

Figure 9. ^{1}H NMR spectra of a 2:1 mixture of **T** and $(\mathbf{D}1)_2\mathbf{B}^{2+}$ in CD_2Cl_2/acetone-d_6 (1:2) at various temperatures. In the spectrum at −55 °C, the ^{1}H NMR signals at δ = 4.253, 4.196, 4.103, and 4.083 ppm were assigned to protons 8-H$_f$, 5-H$_f$, 10-H$_f$, and 3-H$_f$ of the free tweezer by comparison with the ^{1}H NMR spectrum of **T**. The ^{1}H NMR signals at δ = 4.347, 4.235, 4.196, and 4.053 were assigned to the corresponding protons 5-H$_c$, 10-H$_c$, 8-H$_c$, and 3-H$_c$ of complex $(\mathbf{D}1)_2\mathbf{B}^{2+}\cdot\mathbf{T}$ by comparison with the ^{1}H NMR spectrum of $(\mathbf{D}0)_2\mathbf{B}^{2+}\cdot\mathbf{T}$ at −45 °C.

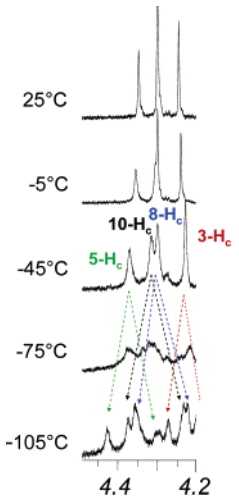

Figure 10. ^{1}H NMR spectra of a 1.2:1 mixture of $(\mathbf{D}1)_2\mathbf{B}^{2+}$ and **T** in CD_2Cl_2/acetone-d_6 (1:2) at various temperatures, representing the shuttling process. Each of the signals in the spectrum at −45 °C at δ = 4.339, 4.230, 4.198, and 4.058, assigned to protons 5-H$_c$, 10-H$_c$, 8-H$_c$, and 3-H$_c$ of the complexed tweezer **T**, is split into two signals by lowering the temperature to −105 °C. At the coalescence temperature of −75 °C, the specific rate constant and the Gibbs activation energy were calculated from the splitting of the signals of 5-H$_c$ ($\delta\nu$ = 125 Hz) to be $k_{coalescence} = \pi\delta\nu/2^{1/2} = 2.22\delta\nu$ = 277 and $\Delta G^{\ddagger}$ = 9.2 kcal/mol.

of the tweezer. In the ^{1}H NMR spectra of the complex $(\mathbf{D}0)_2\mathbf{B}^{2+}\cdot\mathbf{T}$ at temperatures lower than −45 °C (i.e., when dissociation/association proceeds slowly with respect to the NMR time scale), the signals at δ = 8.61, 5.83, and 4.81, assigned to the bipyridinium protons H^o, H^m, and N^+-CH_2, are broadened, but no splitting into separate peaks can be detected. The signal broadening is an indicator for the occurrence of "intramolecular" processes but does not allow us to establish which of these processes is "frozen out on the NMR time scale". However, the specific broadening of the signals assigned to the bridgehead protons 3-, 5-, and 8-H$_c$ of complexed **T** in the ^{1}H NMR spectrum of a 2:1 mixture of **T** and $(\mathbf{D}0)_2\mathbf{B}^{2+}$ at temperatures lower than −45 °C (Figure 7) can only be the result of "freezing out" the shuttling process. The rotational process does not affect the position of these signals. With the assumption that the splitting of signal 5-H$_c$ is $\delta\nu \approx$ 100 Hz in the range of slow exchange, the Gibbs activation energy is of the order of $\Delta G^{\ddagger} \approx$ 9.3 kcal mol^{-1} at −75 °C, the temperature of coalescence. Similar results were obtained for the complex $(\mathbf{D}1)_2\mathbf{B}^{2+}\cdot\mathbf{T}$. In the ^{1}H NMR spectrum of a 1.2:1 mixture of $(\mathbf{D}1)_2\mathbf{B}^{2+}$ and **T** in CD_2Cl_2/acetone-d_6 at −105 °C (Figure 10), the bridgehead protons of complexed tweezer give rise to eight signals. From the splitting of the 5-H$_c$ signals, $\delta\nu$ = 125 Hz, the Gibbs activation energy of the shuttle process can be calculated to be $\Delta G^{\ddagger}$ = 9.2 kcal mol^{-1} at −75 °C, the temperature of coalescence.[37]

(c) Modeling and Structures. The experimentally determined Gibbs activation energies agree well with the energy barrier calculated by force-field MMFF94 for the shuttling process in the complex of tweezer **T** with *N*,*N*-dimethyl-4,4′-bipyridinium dication (Figure 11).[38]

(37) The fact that the averaged signal of each proton (observed in the range of fast exchange) has to be the center of the two signals (observed for each proton in the range of slow exchange) allows the assignment of all bridgehead protons in the spectrum at −105 °C.
(38) *SPARTAN 04*; Wavefunction, Inc.: 18401 Von Karman Ave., Suite 370, Irvine, CA 92715.

The complex structures (Figure 12), which were calculated for the complexes $(\mathbf{D}0)_2\mathbf{B}^{2+}\cdot\mathbf{T}$ and $(\mathbf{D}1)\mathbf{B}^{2+}\cdot\mathbf{T}$ as representative examples by force-field MMFF94,[46] are in good accord with the experimental data. At room temperature these structures are, however, highly dynamic. The tweezer **T** shuttles quickly from one pyridinium ring of the guest molecule to the other, and the guest molecule undergoes a rapid rotation around the long axis of the bipyridinium core inside the tweezer cavity. In the complexes of unsymmetric dendrimers $(\mathbf{D}1)\mathbf{B}^{2+}$ and $(\mathbf{D}2)\mathbf{B}^{2+}$, the ^{1}H NMR signals in CD_2Cl_2 assigned to the protons at the *N*-ethyl-substituted pyridinium ring exhibit larger complexation-induced shifts than those of the corresponding protons at the pyridinium ring substituted with the dendron, whereas in acetone-d_6 these differences in the complexation-induced shifts are small (Table 3). These findings suggest that in the nonpolar solvent, dichloromethane, the *N*-ethyl-substituted pyridinium ring of $\mathbf{D}1\mathbf{B}^{2+}$ and $\mathbf{D}2\mathbf{B}^{2+}$ is preferentially positioned inside the tweezer cavity, whereas in the polar solvent, acetone, such a preference does not exist. This observation is further evidence that in acetone the "intermolecular solvation" can successfully compete with the "intramolecular solvation" resulting from the back-folding of the dendron branches.

The complex formation between the dendrimers and tweezer **T** can be further characterized by the construction of complete Gibbs energy diagrams for the complex dissociation/association by means of the now available thermodynamic and kinetic data (Figure 13). From these diagrams it becomes evident that the formation of the complexes observed here has substantial activation barriers, comparable to the barrier to the formation of the complex between tweezer **T** and 1,2,4,5-tetracyanobenzene (TCNB, $\Delta G^{\ddagger}_{ass}$ = 7.8 kcal mol^{-1}).[35] These barriers are much higher than the barrier expected for diffusion-controlled processes (1−2 kcal mol^{-1} depending on the viscosity of the solution). The Gibbs activation energies determined for the dissociation of the complexes of the symmetric guest molecules $(\mathbf{D}0)_2\mathbf{B}^{2+}\cdot\mathbf{T}$ and $(\mathbf{D}1)_2\mathbf{B}^{2+}\cdot\mathbf{T}$ are of similar size, whereas the

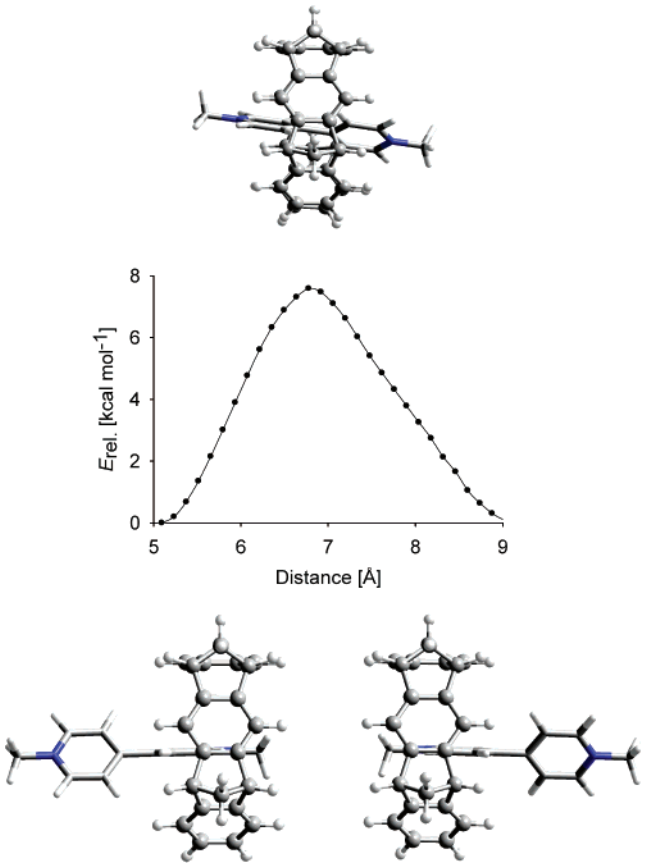

Figure 11. Change in energy, E_{rel}, calculated for the shuttling process of tweezer **T** along the axis of the *N*,*N*-dimethylbipyridinium dication by force-field MMFF 94. "Distance" is given between the *N*-methyl C-atom of the bipyridinium dication and the benzene C-atom fused with the norbornadiene unit of the sidewall of **T** (C-3a). The unsymmetric plot results from the computational method. Thirty structures (which are not completely symmetric) were optimized by force-field calculation with constraints of the distance between 5 and 9 Å given in the plot.

dissociation barrier of the complex of the unsymmetric dendrimer $\mathbf{D}1\mathbf{B}^{2+}\cdot\mathbf{T}$ is smaller by about 2 kcal mol^{-1}. The same trend is found for activation barriers calculated for the association. The stopper groups attached to the bipyridinium core in $(\mathbf{D}0)_2\mathbf{B}^{2+}$ and $(\mathbf{D}1)_2\mathbf{B}^{2+}$ are, evidently, too bulky. Thus, the complex formation and dissociation cannot occur by threading of these guest molecules through the open tweezer face without severe deformation of the tweezer topology (Figure 12). In these cases the complex is formed by moving the guest molecule through the tweezer's tips inside the cavity, as it happens for the association of **T** and TCNB.[35] A further example is the formation of the complex between the benzene-spaced tweezer (Figure 14, **T**, $n = 0$ and R = H) and the bipyridinium salt $(\mathbf{D}0)_2\mathbf{B}^{2+}$.[39] This complex is thermodynamically much less stable than the corresponding complex of the naphthalene-spaced tweezer **T** ($n = 1$) because the inclusion of the guest molecule into the smaller cavity requires a larger expansion of the tweezer sidearms, increasing the strain energy. This strain effect is also responsible for the larger activation barrier of association. The finding of negative entropies of activation for the dissociation of the complexes of **T** with $(\mathbf{D}0)_2\mathbf{B}^{2+}$, $(\mathbf{D}1)_2\mathbf{B}^{2+}$ (Figure 9), and TCNB ($\Delta S^{\ddagger} = -10.6$ cal mol^{-1} K^{-1})[35] suggests that the guest molecule is still clipped between the tweezer's tips in the transition state. The restriction of rotational and translation degrees of freedom in the transition state contributes negative terms to the entropy of activation. The smaller Gibbs activation energies determined for the dissociation/association of the complex with unsymmetric dendrimer $\mathbf{D}1\mathbf{B}^{2+}\cdot\mathbf{T}$ indicate that this complex is formed by a different route than the other complexes, most likely by threading the *N*-ethyl-substituted pyridinium ring of $\mathbf{D}1\mathbf{B}^{2+}$ through the open tweezer face, which can proceed according to force-field calculations (Figure 12) without significant distortion of the tweezer topology.

(39) Kamieth, M.; Klärner F.-G. *J. Prakt. Chem.* **1999**, *341*, No. 3, 245.

Conclusion

The investigation of the spectroscopic and electrochemical behavior of the symmetric and unsymmetric first-, second-, and third-generation dendrimers $(\mathbf{D}n)_2\mathbf{B}^{2+}$ and $\mathbf{D}n\mathbf{B}^{2+}$ ($n = 1, 2, 3$) and their host−guest complexes with tweezer **T** allows the following conclusions to be drawn. The quite strong fluorescence of the 1,3-dimethyleneoxybenzene units of the dendrons is completely quenched as a result of through-bond or through-space donor−acceptor interactions that are also evidenced by a low-energy tail in the absorption spectrum. In dichloromethane solution the 4,4′-bipyridinium cores of the investigated dendrimers are hosted by the molecular tweezer **T**. Host−guest formation causes the quenching of the tweezer fluorescence. The association constants, as measured from fluorescence and ^{1}H NMR titration plots, are of the order of 10^4 M^{-1}, decrease on increasing dendrimer generation, and are slightly larger for the unsymmetric than for the symmetric dendrimer of the same generation. The association constants are strongly solvent-dependent and decrease by more than 1 order of magnitude when the nonpolar solvent, dichloromethane, is replaced by more polar acetone. The large complexation-induced shifts and the temperature dependence of the ^{1}H NMR signals of the host and guest protons provide insight into the structures and dynamics of the host−guest complexes. Accordingly, the bipyridinium core is positioned inside the tweezer cavity with a fast shuttling of the tweezer from one pyridinium ring to the other ($\Delta G^{\ddagger} <$ 10 kcal/mol). In the case of the unsymmetric dendrimers the *N*-ethyl-substituted pyridinium ring is preferentially complexed. The Gibbs activation barriers of the host−guest complex dissociation are in the range of 10.5−13.0 kcal/mol, indicating that the complexation of the bipyridinium dications, which are symmetrically substituted with two bulky stopper groups, proceeds by clipping the guest molecule between the tweezer's tips in the transition state, whereas the complexes of the unsymmetric dendrimers are formed by threading the *N*-ethyl-substituted pyridinium ring through the open tweezer face. Host−guest formation was also found to cause a displacement of the first reduction wave of the 4,4′-bipyridinium unit toward more negative potential values, whereas the second reduction wave was unaffected. These results show that the host−guest complexes between the tweezer and the dendrimers are stabilized by electron donor−acceptor interactions and that they can be reversibly assembled/disassembled by electrochemical stimulation.

Experimental Section

Synthesis of the Molecular Tweezer. The molecular tweezer **T** (Figure 1), comprising a naphthalene and four benzene components

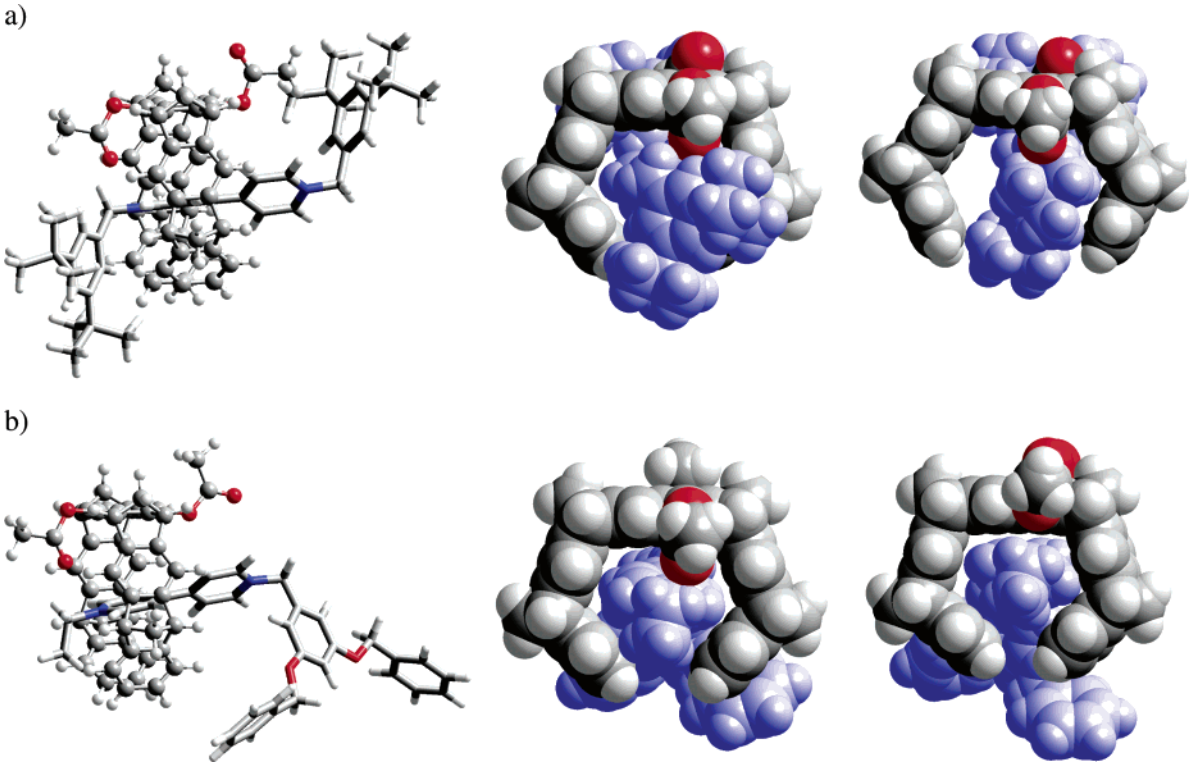

Figure 12. Structures of the complexes (a) $(\mathbf{D}0)_2\mathbf{B}^{2+}\cdot\mathbf{T}$ and (b) $\mathbf{D}1\mathbf{B}^{2+}\cdot\mathbf{T}$. Left, side view (ball-and-stick); center, top view (space-filling); right, top view on the transition state of dissociation by threading (space-filling). The sidearms of tweezer **T** have to be substantially expanded in the transition state of dissociation of $(\mathbf{D}0)_2\mathbf{B}^{2+}\cdot\mathbf{T}$, whereas the dissociation of $\mathbf{D}1\mathbf{B}^{2+}\cdot\mathbf{T}$ can proceed without significant distortion of the tweezer geometry.

bridged by four trimethylene units, was prepared and characterized as previously described.[40]

Synthesis of the Symmetric Dendrimers. The preparation of the symmetric $(\mathbf{D}n)_2\mathbf{B}^{2+}$ dendrimers (Figure 1) as PF_6^- salts in a pure form has already been reported.[27]

Synthesis of the Unsymmetric Dendrimers. The unsymmetric $\mathbf{D}n\mathbf{B}^{2+}$ dendrimers were obtained by reacting $\mathbf{B}Et^+$ (Figure 14), prepared as the PF_6^- salt,[41] with the **D**1**Br**, **D**2**Br**, and **D**3**Br** dendrons (Figure 14), prepared according to the previously described literature procedure.[42]

The solvents were dried using standard techniques prior to use. All reactions were performed in standard glassware under an inert argon atmosphere. Thin-layer chromatography (TLC) was carried out on TLC plates precoated with RP-18 F_{254}'s (Merck 1.15685). Medium-pressure liquid chromatography (MPLC) was carried out with a Büchi pump using Merck RP 18 (15−25 μm). Melting points were determined on a Reichert Thermovar microscope and were not corrected. ^{1}H NMR and ^{13}C NMR spectra were recorded using Bruker instruments (Avance 300 and AM 400). Mass spectra were recorded using a MS-50 from A.E.I., Manchester, GB (EI), a Concept 1H from Kratos Analytical Ltd., Manchester, GB (FAB), and a MALDI-TofSpec-E from Micromass, GB.

D1B(PF$_6$)$_2$. A solution of **B**EtPF$_6$ (3.30 g, 10.0 mmol) and **D**1**Br** (4.98 g, 13.0 mmol) in dry *N*,*N*′-dimethylformamide (20 mL) was heated at 70 °C for 7d. The solid that formed was filtered, washed several times with dichloromethane, and dried. The crude product was then suspended in water (20 mL), and the resulting precipitate was filtered off. A solution of aqueous NH_4PF_6 (2 mL, 50%) was added to the filtrate, and the solid that was produced was filtered, washed several times with water, and dried to yield **D**1**B**(PF$_6$)$_2$ as a colorless solid (883 mg, 11%): mp 200−204 °C; ^{1}H NMR (300 MHz, DMSO-d_6, 25 °C) δ 1.60 (t, $^3J_{HH}$ = 7 Hz, 3 H; CH_3), 4.77 (q, $^3J_{HH}$ = 7 Hz, 2 H; N^+CH_2), 5.11 (s, 4 H; OCH_2), 5.91 (s, 2 H; N^+CH_2), 6.72 (s, 1 H; H_{ar}), 7.00 (s, 2 H; H_{ar}), 7.29 (d, $^3J_{HH}$ = 7 Hz, 2 H; H_{ar}), 7.36 (t, $^3J_{HH}$ = 7 Hz, 4 H; H_{ar}), 7.42 (d, $^3J_{HH}$ = 7 Hz, 4 H; H_{ar}), 8.82 (m, 4 H; H_{py}), 9.46 (d, $^3J_{HH}$ = 7 Hz, 2 H; H_{py}), 9.63 (d, $^3J_{HH}$ = 7 Hz, 2 H; H_{py}); ^{13}C NMR (75 MHz, DMSO-d_6, 25 °C) δ 16.3, 56.5, 63.0, 69.6, 102.5, 108.3, 126.7, 127.0, 127.8, 127.9, 128.4, 136.1, 136.6, 145.5, 145.7, 148.5, 149.0, 159.9; FAB-MS m/z = 633.2 [M − PF$_6$]$^+$.

D2B(PF$_6$)$_2$. A solution of **B**EtPF$_6$ (1.02 g, 3.08 mmol) and **D**2**Br** (3.23 g, 4.00 mmol) in dry *N*,*N*′-dimethylformamide (20 mL) was heated at 70 °C for 7 d. The solvent was evaporated and the crude product extracted with water. The solid was filtered off, dried, and recrystallized from acetone. The crude product was then suspended in water (60 mL), heated at 80 °C for several minutes, and filtered hot, and to the hot filtrate was added aqueous NH_4PF_6 (4 mL, 50%). The arising solid was filtered and dried and yielded **D**2**B**(PF$_6$)$_2$ as an orange-colored solid (947.0 mg, 26%): mp 95−96 °C; ^{1}H NMR (300 MHz, acetone-d_6, 25 °C) δ 1.63 (t, $^3J_{HH}$ = 7 Hz, 3 H; CH_3), 4.83 (q, $^3J_{HH}$ = 7 Hz, 2 H; N^+CH_2), 4.98 (s, 12 H; OCH_2), 5.92 (s, 2 H; N^+CH_2), 6.52 (t, $^4J_{HH}$ = 2 Hz, 2 H; H_{ar}), 6.60 (d, $^4J_{HH}$ = 2 Hz, 4 H; H_{ar}), 6.69 (t, $^4J_{HH}$ = 2 Hz, 1 H; H_{ar}), 6.81 (d, $^4J_{HH}$ = 2 Hz, 2 H; H_{ar}), 7.18−7.29 (m, 12 H; H_{ar}), 7.33 (m, 8 H; H_{ar}), 8.60 (m, 4 H; H_{py}), 9.21 (d, $^3J_{HH}$ = 7 Hz, 2 H; H_{py}), 9.29 (d, $^3J_{HH}$ = 7 Hz, 2 H; H_{py}); ^{13}C NMR (75 MHz, acetone-d_6, 25 °C) δ 16.7, 58.7, 65.7, 70.4, 70.6, 102.2, 104.1, 107.4, 109.4, 128.1, 128.3, 128.5, 128.7, 129.3, 135.9, 138.2, 140.3, 146.4, 146.8, 150.7, 151.4, 161.1, 161.7; FAB-MS m/z = 1057.3 [M − PF$_6$]$^+$.

D3B(PF$_6$)$_2$. A solution of **B**EtPF$_6$ (0.51 g, 1.54 mmol) and **D**3**Br** (3.31 g, 2.00 mmol) in dry *N*,*N*′-dimethylformamide (20 mL) was heated at 70 °C for 7 d. The solvent was evaporated, and the crude product was extracted with water and dried. A suspension of the crude product in acetonitrile (0.1 M NH_4PF_6)/water (20 mL, 25:2) was heated at 80 °C for several minutes and cooled to room temperature, and the resulting solid was filtered. Purification by MPLC (RP 18; acetonitrile (NH_4PF_6 0.1 mol)/dichloromethane 25:2) gave **D**3**B**(PF$_6$)$_2$ as an orange-colored

(40) Klärner, F.-G.; Burkert, U.; Kamieth, M.; Boese, R. *J. Phys. Org. Chem.* **2000**, *13*, 604.
(41) (a) Ashton, P. R.; Ballardini, R.; Balzani, V.; Constable, E. C.; Credi, A. *Chem Eur. J.* **1998**, *4*, 2413. (b) Minisci, F.; Bertini, F.; Galli, R.; Quilico, A. Ger. Offen. 2 153 234/1972.
(42) Hawker, C. J.; Fréchet, J. M. J. *J. Am. Chem. Soc.* **1990**, *112*, 7638.

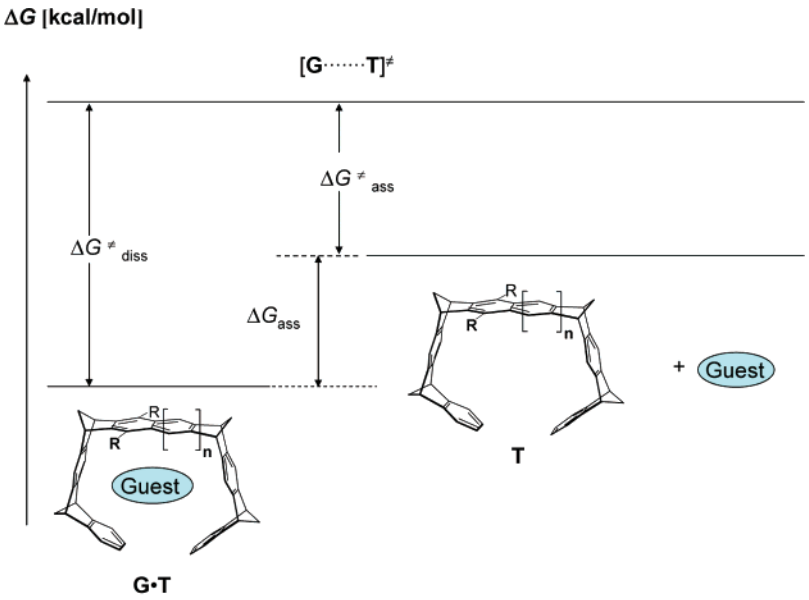

Complex	$\Delta G^{\neq}_{diss}$	ΔG_{ass}	$\Delta G^{\neq}_{ass}$
$(\mathbf{D}0)_2\mathbf{B}^{2+}\bullet\mathbf{T}$	12.6 [b),f)]	-3.9 [b)]	8.7 [b)]
	13.0 [c),e)]	-5.4 [c)]	7.6 [c)]
$(\mathbf{D}1)_2\mathbf{B}^{2+}\bullet\mathbf{T}$	12.0 [d),f)]	-4.4 [d)]	7.6 [d)]
$\mathbf{D}1\mathbf{B}^{2+}\bullet\mathbf{T}$	10.5 [d),e)]	-4.3 [d)]	6.2 [d)]
$(\mathbf{D}0)_2\mathbf{B}^{2+}\bullet\mathbf{T}$(n=0, R=H)	12.0 [b),e)]	-2.4 [b)]	9.6 [b)]

Figure 13. Gibbs activation energy diagram of association and dissociation for the complex formation between tweezer **T** and guest molecules $(\mathbf{D}0)_2\mathbf{B}^{2+}$, $(\mathbf{D}1)_2\mathbf{B}^{2+}$, and $\mathbf{D}1\mathbf{B}^{2+}$. [a] $\Delta G^{\ddagger}_{ass} = \Delta G^{\ddagger}_{diss} + \Delta G_{ass}$. [b] In $CDCl_3$/acetone-d_6 (1:2). [c] In CD_2Cl_2. [d] In CD_2Cl_2/acetone-d_6 (1:2). [e] Calculated from the differences in resonance frequencies at the coalescence temperature. [f] Determined by line shape analysis.

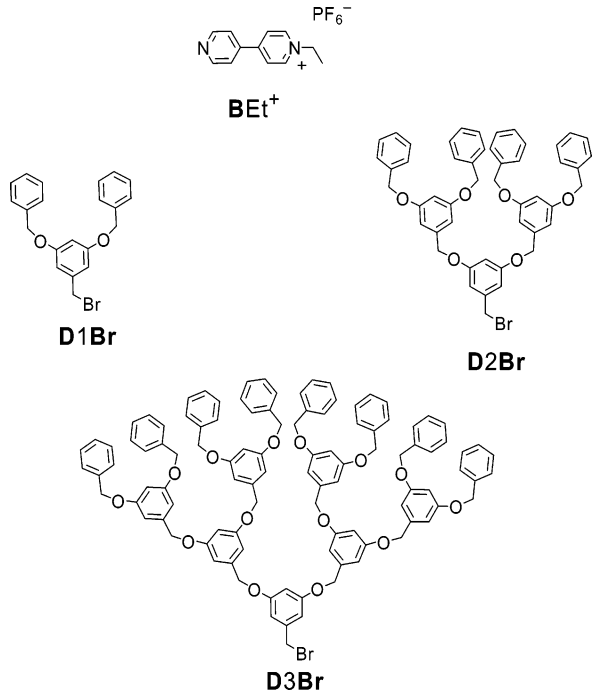

Figure 14. Starting compounds in the synthesis of unsymmetric dendrimers.

amorphous solid (220 mg, 7%): ^{1}H NMR (300 MHz, $CDCl_3$, 25 °C) δ 1.12 (t, $^3J_{HH}$ = 7 Hz, 3 H; CH_3), 3.98 (q, $^3J_{HH}$ = 7 Hz, 2 H; N^+-CH_2CH_3), 4.72 (2s, 28 H; OCH_2), 5.10 (s, 2 H; N^+CH_2), 6.37 (m, 7 H; H_{ar}), 6.49 (m, 14 H; H_{ar}), 7.06−7.20 (m, 40 H; H_{ar}), 7.71 (m, 4 H; H_{py}), 8.10 (d, $^3J_{HH}$ = 6 Hz, 2 H; H_{py}), 8.25 (d, $^3J_{HH}$ = 6 Hz, 2 H; H_{py}); ^{13}C NMR (75 MHz, $CDCl_3$, 25 °C) δ = 15.6, 57.6, 65.0, 69.8, 70.1, 70.3, 101.3, 101.8, 102.5, 106.6, 106.7, 107.5, 126.9, 127.7, 127.9, 128.1, 128.7, 136.9, 139.1, 139.4, 139.5, 144.4, 144.7, 149.4, 150.0, 160.1, 160.2, 160.8; FAB-MS m/z = 1906.6 $[M - PF_6]^+$.

Determination of K_a by ^{1}H NMR Titration. Host H and guest G are in equilibrium with the 1:1 complex HG. The association constant K_a is then defined by eq 1. $[H]_0$ and $[G]_0$ are the starting concentrations of host and guest, respectively.

$$K_a = \frac{[HG]}{[H][G]} = \frac{[HG]}{([H]_0 - [HG])([G]_0 - [HG])} \quad (1)$$

The observed chemical shift δ_{obs} of the guest proton in the ^{1}H NMR spectrum (Bruker Instruments DRX 500, 500 MHz, 25 °C) of a host and guest mixture is an averaged value between free (δ_0) and complexed guest (δ_{HG}), in the case of the exchange between free and complexed guest being fast with respect to the NMR time scale (eq 2). Combination of eqs 1 and 2 and the use of differences in chemical shift ($\Delta\delta = \delta_0 - \delta_{obs}$; $\Delta\delta_{max} = \delta_0 - \delta_{HG}$) lead to eq 3.

$$\delta_{obs} = \frac{[G]}{[G] + [HG]}\delta_0 + \frac{[HG]}{[G] + [HG]}\delta_{HG} \quad (2)$$

$$\Delta\delta = \frac{\Delta\delta_{max}}{[G]_0}\left(\frac{1}{2}\left([H]_0 + [G]_0 + \frac{1}{K_a}\right) - \sqrt{\frac{1}{4}\left([H]_0 + [G]_0 + \frac{1}{K_a}\right)^2 - [H]_0[G]_0}\right) \quad (3)$$

Two types of titration experiments were performed: (i) in the case of $K_a \leq 1000\ M^{-1}$, the total guest concentration $[G]_0$ was kept constant, whereas the total host concentration $[H]_0$ was varied; (ii) in the case of $K_a > 1000\ M^{-1}$, dilution titrations were performed on solutions containing equimolar amounts of host and guest with concentrations in the range between 0.5 and 4 mM. In both experiments $\Delta\delta$ was determined as the difference of the chemical shifts of the proton of pure guest (δ_0) and of the guest in the various host−guest mixtures (δ_{obs}). The dependence of δ_{obs} on the host concentrations afforded the data pairs $\Delta\delta$ and $[H]_0$. Fitting of these data to the 1:1 binding isotherm by iterative methods delivered the parameters K_a and $\Delta\delta_{max}$.[43] Since our guest molecules possess more than one kind of nonequivalent protons, K_a and $\Delta\delta_{max}$ were determined for each guest proton, and the average of all K_a values is given in Table 2. In a few cases, the guest proton signals cannot be unambiguously assigned because they are broadened or superimposed by other NMR signals. The $\Delta\delta_{max}$ values of these guest protons were calculated by the use of eq 4. The experimental error was estimated to be small for the $\Delta\delta_{max}$ values (<5%) but larger for the binding constants K_a (≤20%), particularly in the case of the highly stable complexes for which these data have to be determined by NMR dilution titrations (see Supporting Information).

$$\Rightarrow \Delta\delta_{n,max} = \Delta\delta_n \frac{\Delta\delta_1}{\Delta\delta_{1,max}} \quad (4)$$

Determination of the Activation Parameters $\Delta H^{\ddagger}$, $\Delta S^{\ddagger}$, and $\Delta G^{\ddagger}$ by ^{1}H NMR Line Shape Analysis. The exchange frequencies k of the dynamic processes are determined from the line shapes of the exchanging ^{1}H NMR signals of the tweezer in different solvent mixtures ($CDCl_3$/acetone-d_6 1:2 and CD_2Cl_2/acetone-d_6 1:2) by simulation of these signals with the computer program WINDYNA.[44] The activation parameters are derived from the temperature dependence of k by the use of the Arrhenius equation and the Eyring transition-state theory (eqs 5−8).

$$k = A \exp\left(-\frac{E_a}{RT}\right) \quad (5)$$

$$\Delta S^{\ddagger} = R\left(\ln A - \ln\left(\frac{k_B T}{h}\right) - 1\right) \quad (6)$$

$$\Delta H^{\ddagger} = E_a - RT \quad (7)$$

$$\Delta G^{\ddagger} = \Delta H^{\ddagger} - T\Delta S^{\ddagger} \quad (8)$$

Photophysical Measurements. The absorption spectra and the photophysical properties (emission spectra, emission quantum yields, and excited-state lifetimes) have been studied at room temperature (293 K) in dichloromethane or acetonitrile/dichloromethane (1:1 v/v) air-equilibrated solutions. The equipment used has been described elsewhere.[45] Fluorescence quantum yields were measured following the methods of Demas and Crosby[46] (standard used: terphenyl in cyclohexane, $\Phi = 0.82$).[47] The association constants were obtained from fluorescence titration experiments. The estimated experimental error is 2 nm on the band maximum, 5% on the molar extinction coefficient, 10% on the fluorescence quantum yield, and 5% on the fluorescence lifetime.

Electrochemical Study. The electrochemical experiments were carried out at room temperature in argon-purged dichloromethane/acetonitrile (9:1 or 3:1 v/v) mixtures with 0.1 M tetrabutylammonium hexafluorophosphate ($[NBu_4]PF_6$) as supporting electrolyte by an EcoChemie Autolab 30 multipurpose instrument interfaced to a personal computer. In the cyclic voltammetry the working electrode was a glassy carbon electrode (0.08 cm^2, Amel), the counter electrode was a Pt spiral, separated from the bulk solution by a fine glass frit, and a silver wire was employed as a quasi-reference electrode (AgQRE). All the potentials reported are referred to SCE by measuring the AgQRE potential with respect to ferrocene. Cyclic voltammograms were obtained with scan rates in the range $0.02-5\ V\ s^{-1}$. The number of exchanged electrons in each wave is estimated by comparison with the wave of the one-electron oxidation of ferrocene.

Acknowledgment. We thank Professors Mauro Maestri and Margherita Venturi for useful discussions. This work was supported by MIUR (Supramolecular Devices Project) and Deutsche Forschungsgemeinschaft.

Supporting Information Available: Additional experimental and characterization details. This material is available free of charge via the Internet at http://pubs.acs.org.

JA056615J

(43) A nonlinear regression analysis of eq 3 was performed by the use of the program Table Curve 4.0, SPSS Science, analogous to the computer program HOSTEST by C. S. Wilcox and N. M. Glagovich, University of Pittsburgh, and the program Associate V1.6, B. Peterson, Ph.D. Dissertation, University of California at Los Angeles, 1994.
(44) *WINDYNA*, v. 1.01; Bruker Daltonik GmbH: 1998.
(45) Bergamini, G.; Ceroni, P.; Balzani, V.; Vögtle, F.; Lee, S.-K. *ChemPhysChem* **2004**, *5*, 315.
(46) Demas, J. N.; Crosby, G. A. *J. Phys. Chem.* **1971**, *75*, 991.
(47) Berlman, I. B. *Handbook of Fluorescence Spectra of Aromatic Molecules*, 2nd ed.; Academic Press: New York, 1971.